Available online at www.scholarsresearchlibrary.com

Scholars Research Library

Scholars Research Library

Archives of Applied Science Research, 2010, 2 (2): 127-135

(http://scholarsresearchlibrary.com/archive.html)

ISSN 0975-508X
CODEN (USA) AASRC9

Dielectric study of Tin oxide nanoparticles at low temperature

A. S. Lanje[1*], S. J. Sharma[2], R. B. Pode[3]and R. S. Ningthoujam[4]

[1]*Department of Electronics, Dr. Ambedkar College, Chandrapur, India*
[2]*Department of Electronics, R. T. M. Nagpur University, Nagpur, India*
[3]*Department of Physics, Kyung Hee University, Seoul, Korea*
[4]*Chemistry Division, Bhabha Atomic Research Center, Mumbai, India*

Abstract

Nanoparticles of SnO_2 have been prepared by co-precipitation method using $SnCl_2$ as a precursor and subsequent heat-treatment at 600°C. X-ray diffraction (XRD) study reveals tetragonal structure of SnO_2 nanopartcles without any secondary phase. Scanning electron microscopy (SEM) image shows the spherical grain morphology of SnO_2 nanopaticles. In transmission electron microscopy (TEM) study of SnO_2, particle size is found to be 25 nm, which is close to crystallite size (21 nm) from XRD using Scherrer equation. In Fourier transform infrared (FTIR) study, a broad peak centered around 650 cm^{-1} was observed due to Sn-O vibration. Frequency dependence dielectric anomaly is observed in SnO_2 nanoparticles at low temperature. Capacitance and loss tangent are found to be decrease with increasing frequency and increase with increasing temperature.

Key words: dielectric, nanoparticles, tin oxide, precipitation.

INTRODUCTION

High-transparency semiconductors such as SnO_2 and In_2O_3 have potential applications in flat panel displays and gas sensors, etc [1-8]. Particularly, bulk SnO_2 has wide band-gap (E_g) of 3.6 eV and thin films can have high conductivity depending on oxygen vacancy [5]. SnO_2 has been synthesized by different methods such as the sol–gel method [9], chemical vapor deposition (CVD) [10], magnetron sputtering [11] and hydrothermal treatment [12]. The electrical conductivity and luminescence properties of SnO_2 are mainly decided by the oxygen vacancy present in SnO_2 lattice [13]. Electrical and optical properties of SnO_2 nanoparticles alter due to their high surface to volume ratio. The study of dielectric properties and a. c. electrical conductivity throws light on the behavior of charge carriers under an a. c. field, their mobility and the mechanism of conduction [14-17].

In this paper, we have synthesized SnO_2 nanoparticles by co-precipitation method using stannous chloride as a precursor, ammonia solution as a precipitating agent and carbon black powder as

reducing agent. With this method, we can prepare SnO_2 nanoparticles in large amount with low cost precursors. Dielectric properties of SnO_2 particles at low temperature (85-300 K) are studied.

MATERIALS AND METHODS

Synthesis

All chemicals used in the experiment were analytic reagent (AR) grade. Stannous chloride ($SnCl_2.2H_2O$) was purchased from Glaxo SmithKline Pharmaceutical Ltd. Ammonia solution (25 %) and carbon black powder were purchased from Merck, India. All chemicals were used as received without further purification. Deionized water was used during the reaction.

In preparation of SnO_2, 2 g (0.1 M) of stannous chloride dihydrate is dissolved in 100 ml water. After complete dissolution, about 4 ml ammonia solution is added to above aqueous solution with stirring. Stirring is continued for 20 minutes. White gel precipitate is immediately formed. It is allowed to settle for 12 h. Then it is filtered and washed with water 2-3 times. 0.27 g carbon black powder (charcoal activated) is mixed with filtered precipitate. The obtained mixer is dried for 24 h at 70 ºC. Dried powder is crushed and heated at 600 ºC for 4 h.

Characterization techniques

The powder X-ray diffraction (XRD) is recorded using Philips Holland, XRD system PW 1710 with nickel filtered CuK_α (λ = 1.5405 Å) radiation. The average crystallite size (t) has been calculated from the line broadening using the Scherrer's relation: $t = 0.9\lambda/B\cos\theta$, where, λ is the wavelength of X-ray and B is the half maximum line width. Scanning electron microscopy (SEM) is performed by JEOL JSM -5600. The transmission electron microscopy (TEM) is performed with Tecnai 20 G^2 under 200 KV. Samples are prepared by dispersing drop of colloid on copper grid, covered with the carbon film and the solvent is evaporated. To record Fourier transform infrared (FTIR) spectra, Bomem Hartmann & Braun MB Series Infrared spectrometer is used. SnO_2 powder is crushed with KBr particles (1:5) and pressed into thin pellets. Dielectric measurements at low temperature are performed by HP 4192A LF Impedance Analyzer (5 Hz-13 MHz) with fully automated dielectric measurement set up.

RESULTS AND DISCUSSION

Structural and particle size studies

XRD pattern of SnO_2 nanoparticles prepared at 600 °C are shown in figure 1. All the peaks of XRD belong to tetragonal lattice of SnO_2. The lattice parameters are calculated by using program Unit Cell - method of TJB Holland & SAT Redfern 1995. The calculated lattice parameters of SnO_2 are a = 4.723(1) Å, c = 3.238(1) Å and its unit cell volume is V = 72.24 $Å^3$ and these values are well agreement with the reported values (JCPDS file No. 71-0652). The peaks are broad due to the nano-size effect. No trace of secondary phase is found. The crystallite size of SnO_2 nanoparticles is found to be 21 nm by using scherrer formula (FWHM).

Figure 2 shows SEM image of prepared SnO_2 nanoparticles. The spherical grain morphology of SnO_2 nanoparticles is observed. Figure 3 shows TEM micrograph of SnO_2 nanoparticles (scale 20 nm) prepared at 600 °C. The average grain size obtained from TEM microstructure is nearly 25 nm. It is slightly greater than crystallite size obtained from XRD analysis (21 nm) using Scherrer's formula. Inset of figure 3 shows its selected area electron diffraction (SAED) pattern. From this tetragonal patterns of spots are observed indicating the high crystallinity of particles.

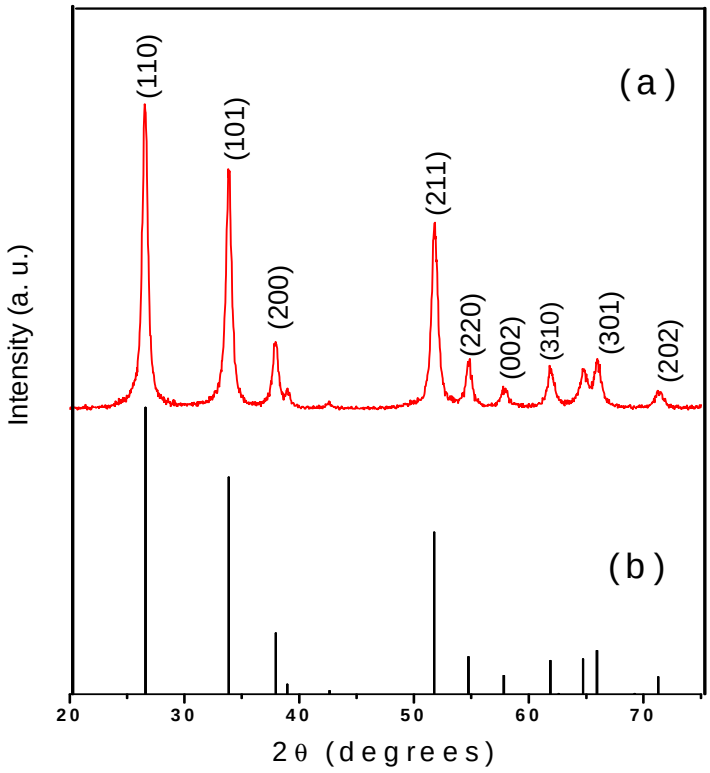

Figure 1. XRD pattern of SnO_2 nanoparticles

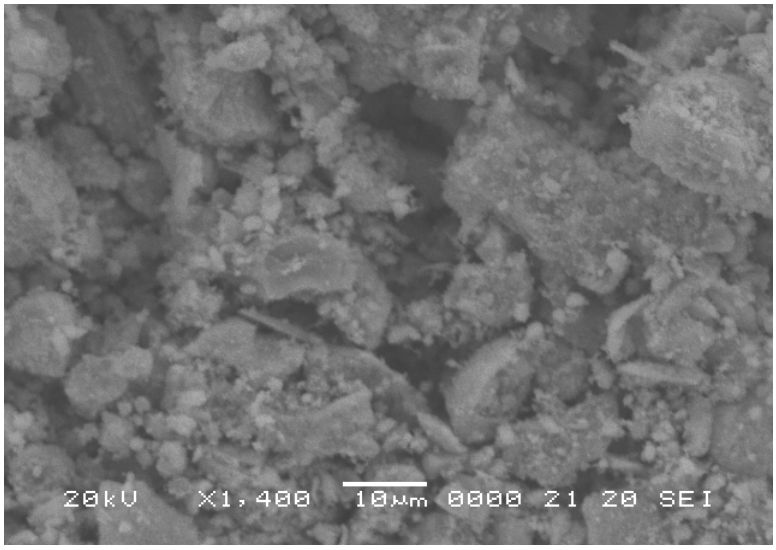

Figure 2. SEM image of SnO_2 nanoparticles

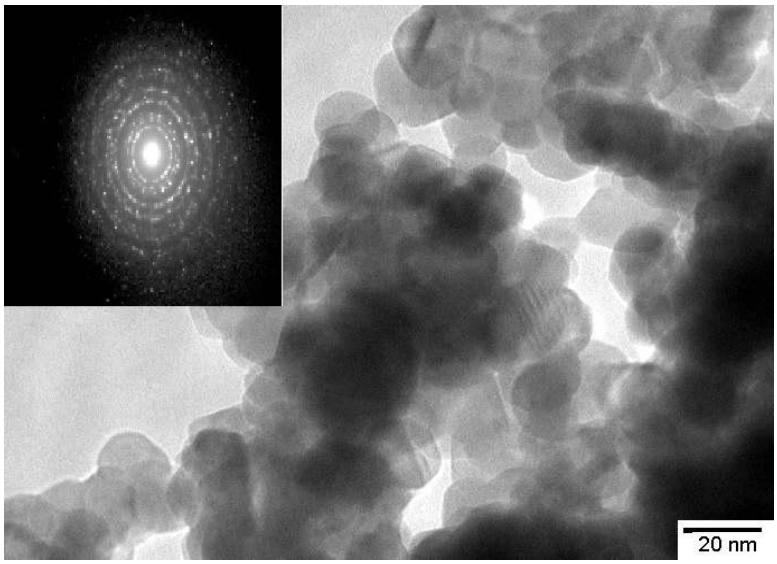

Figure 3. TEM image of SnO_2 nanoparticles. Inset figure shows SAED pattern

FTIR study

FTIR spectra of SnO_2 nanoparticles prepared at 600 °C are shown in figure 4. The broad peak centered at 650 cm^{-1} is observed. The broad band between 800 and 500 cm^{-1} was due to the vibrations of Sn-O [18, 19]. Remaining peaks at 1600 and 3435 cm^{-1} are due to absorption of water during preparation of IR pellet.

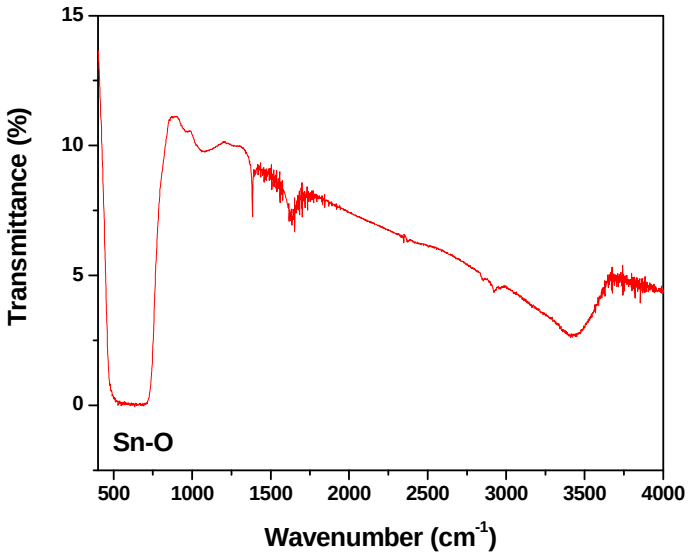

Figure 4. FTIR of SnO_2 nanoparticles

Dielectric measurement

The dielectric studies of SnO_2 carried out by using a dielectric cell and an impedance analyzer (model: HP 4192A). The 10 mm in diameter disc shaped samples is used to find out the dielectric constant. The capacitance and dielectric loss in the frequency range 10 KHz –1 MHz are found out. Dielectric constant or relative permittivity is calculated by using the formula:

$$\varepsilon_r = \frac{C \times d}{\varepsilon_0 A}$$

where, *d* is the thickness of the sample, *C* the capacitance and *A* the area of cross section of the sample. ε_r is the relative permittivity of the material which is a dimensionless quantity. ε_0 is the dielectric permittivity of vacuum (8.854 x 10^{-12} F/m). From these measurements ε_r and $\tan\delta$ (dielectric loss factor) are made available for the evaluation of a. c. conductivity.

Figure 5 shows the variation of dielectric constant and loss with frequency at temperature 300 K. The dielectric constant decreases fast with frequency up to 100 KHz. But after 100 KHz it remains almost constant. The variation of dielectric loss with frequency shows dielectric loss decreases exponentially up to 10 KHz. There is a large hump between frequency 10 KHz to 1000 KHz. The value of dielectric constant (ε_r) of SnO_2 nanoparticles is very high as compare to that of bulk SnO_2 which is reported at room temperature [20].

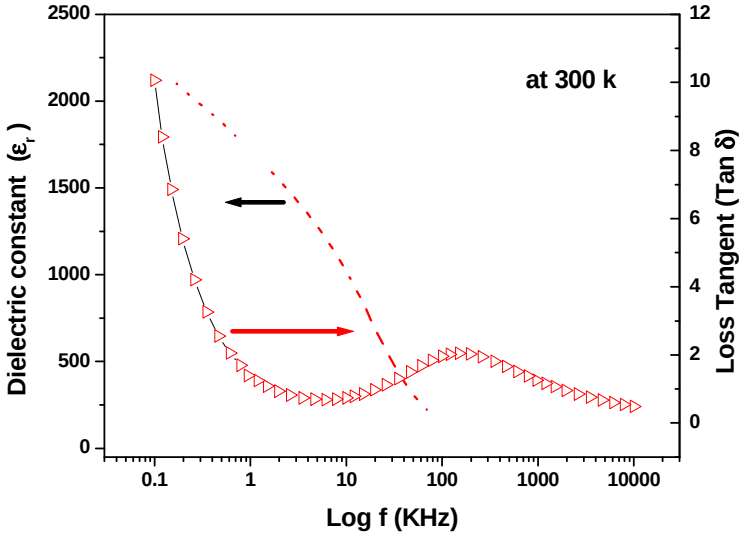

Figure 5. Frequency dependent dielectric variations of SnO_2 at 300 K

It is well known that there are two dielectric polarization mechanisms that contribute to the enhanced dielectric behavior of nanomaterials: rotation direction polarization (RDP) process and space charge polarization (SCP) process. We suggest that both RDP and SCP process contribute to the enhancement of dielectric response of the SnO_2 nanoparticles. First, RDP process is an important contribution for the higher ε_r of the SnO_2 nanoparticles. As for the typical n-type semiconductor, there are a large amount of oxygen vacancies acting as shallow donors in SnO_2, resulting in a lot of oxygen vacancies existing in the interfaces of SnO_2 nanoparticles [21, 22]. Positive oxygen vacancies together with negative oxygen ions give a large amount of dipole moments. These dipole moments will rotate in an external electric field, which leads to the rotation direction polarization occurring in the interfaces of n-type SnO_2 nanoparticles. On the other hand, SCP process can also occur in the sample. Generally, nanostructured materials have about 10^{19} interfaces/cm^3, much more than those of bulk solids [20]. The interfaces with a large volume fraction in the nanostructure sample compacted under high pressure (50 MPa) contain a large amount of defects, such as micro porosities, dangling bonds and vacancy clusters. These defects can cause a change of positive and negative space charge distributions in interfaces [23, 24]. Negative and positive space in interfaces move towards positive and negative poles of the electric field respectively. As they are trapped by defects, dipole moments will form and SCP process will occur in the sample. Because the volume fraction of the interfaces of nano-size

sample is larger than that of bulk materials, SCP is stronger than that in the bulk materials. Thus, ε_r of the SnO_2 nanoparticles is higher than that of bulk. Nevertheless, in the high frequency range, dielectric response of RDP and SCP cannot keep up with the electrical field frequency variation, resulting in the rapid decrease of ε_r in SnO_2 nanoparticles.

Figure 6 shows the temperature frequency dependent of dielectric constant (ε_r) for SnO_2 nanoparticles. It shows that the dielectric constant (ε_r) remains almost constant up to temperature 200 K but it increases with temperature after 200 K. This phase transformation temperature occurs depending on frequency. The ε_r increases with temperature but decreases with frequency. The maximum values of dielectric constant are decreases with increasing frequency. As the temperature increases, the dipoles comparatively become free and they respond to the applied electric field. Thus polarization increased and hence dielectric constant is also increased with the increase of temperature [25].

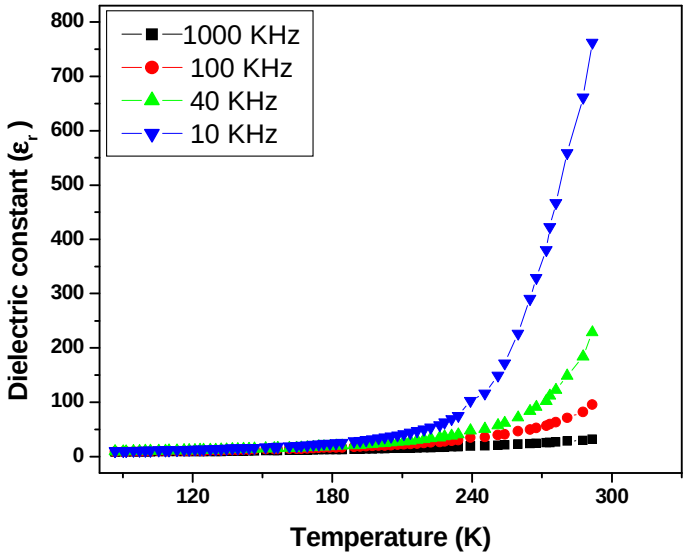

Figure 6. Variations of dielectric constant with temperature at different frequencies for SnO_2 nanoparticles

Figure 7 shows the temperature frequency dependence of dielectric loss for SnO_2. Loss tangent increases with increase in frequency. It shows an anomaly after 245 K depending on frequency. Maxima dielectric loss increases with frequency. Phase transition also increases with frequency.

The a. c. conductivity of SnO_2 (σ_{ac}) is calculated with the data available from dielectric measurement and by using the relation:

$$\sigma_{ac} = 2\pi f \tan\delta\varepsilon_0\varepsilon_r$$

Where, f is the frequency of applied field, $tan\ \delta$ is loss tangent available from dielectric measurement, ε_r is the relative permittivity of the sample and ε_0 is the dielectric permittivity of vacuum (8.854 x 10^{-12} F/m). Table I shows the maximum values of ε_r and σ_{ac} at 300 K for SnO_2 at various frequencies.

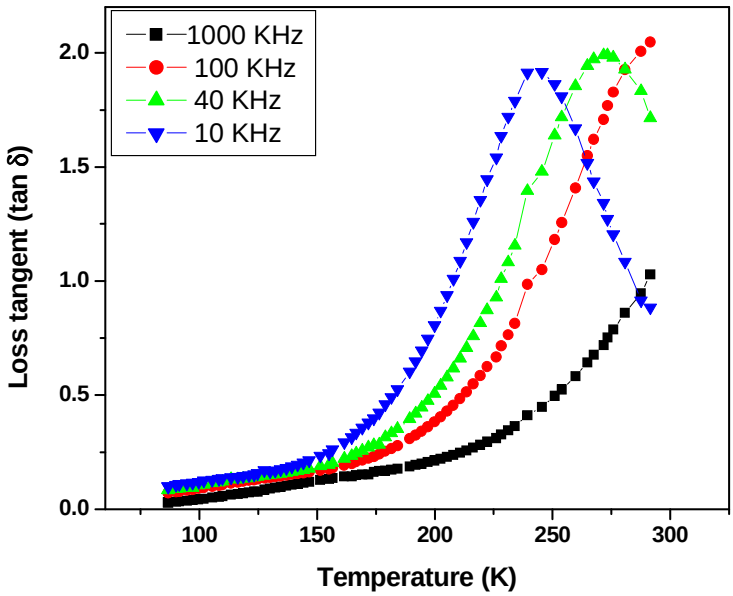

Figure7. Variations of dielectric loss with temperature at different frequencies for SnO_2 nanoparticles

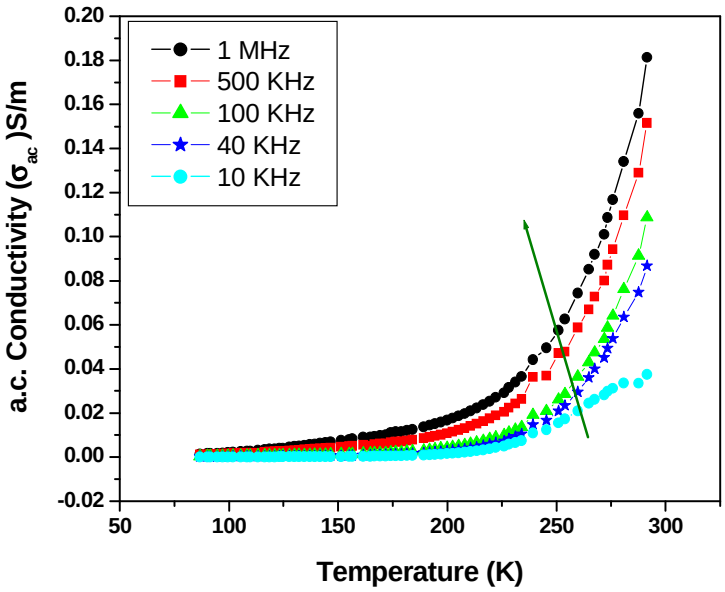

Figure 8. Variation of a. c. conductivity with temperature in SnO_2 nanoparticles

Table I. The maximum values of ε_r and σ_{ac} at 300 K for SnO_2 at various frequencies

Frequency (KHz)	Dielectric constant (ε_r)	a. c conductivity (σ_{ac}) 10^{-5} S/m
10	762.5	0.037
40	228.3	0.086
100	95.8	0.1
1000	31.8	0.181

Figure 8 shows the temperature frequency dependence of a. c. conductivity. It is observed that a. c. conductivity increases with increase in temperature, indicating mobility of charge carriers responsible for hopping. As temperature increases, mobility of hopping ions increases thereby increasing conductivity. The a. c. conductivity also increases with increasing frequency. The electrons which are involved in hopping are responsible for electronic polarization in SnO_2 [26-27].

CONCLUSION

Tin oxide (SnO_2) nanoparticles of 25 nm average size are prepared successfully. Dielectric constant of SnO_2 nanoparticles is found to be larger than that of bulk due to larger volume fraction of the interfaces and stronger SCP of nanoparticles. Dielectric constant and dielectric loss decreases with frequency at low temperature and increases with temperature. Dielectric loss shows an anomaly at around 250 K depending on frequency due to nano-size of the particles. The a. c. conductivity increases with temperature indicating mobility of charge carriers responsible for hopping. As temperature increases mobility of hopping ions increases thereby increasing conductivity.

Acknowledgments
One of authors (ASL) would like to acknowledge financial support from UGC, New Delhi, for present research work. The authors are grateful to Dr. Ajay Gupta, Dr. N. P. Lalla, Dr. D. M. Phase and Dr. A. Banerjee, UGC-DAE Consortium for Scientific Research Center, Indore for providing SEM, TEM and dielectric measurements facilities. Authors thank Dr. D. Das, Chemistry Division, Bhabha Atomic Research Center, Mumbai for providing facility of FTIR. Thanks are also extended to Dr. R. R. Dahegaonkar for providing laboratory facilities.

REFERENCES

[1] RS Ningthoujam; SK Kulshreshtha. *Mater. Res. Bull.*, **2008**, 104, 123906.
[2] R Khandelwal; AP Singh; A Kapoor; S Grigorescu; P Miglietta; NE Stankova; Perrone. *Opt. Laser Technol.,* **2009,** 41, 89.
[3] V Vasu ; A Subramanyan. *Thin Solid Films*, **1990**,193, 973.
[4] J Ni; X Zhao; X Zheng; J Zhao; B Liu. *Acta. Mater.*, **2009**, 57, 278.
[5] C Kilic; A Zunger. *Phys. Rev. Lett.*, **2002**, 88, 95501.
[6] YI Lee; KJ Lee; DH Lee; YK Jeong; HS Lee; YH Choa. *Curr. Appl. Phys.*, **2009**, 9, S79.
[7] C Bouzidi; H. Elhouichet; A Moadhen; M Oueslati. *J. Lumin.*, **2009**, 29, 30.
[8] AL Dawar; JC Joshi. *J. Mater. Sci*, **1984**, 19, 1.
[9] R Rella; A Serra; P Siciliano. *Sens. Actuators*, **1997**, B 44.
[10] SC Ray; MK Karanjai; D Dasgupta. *Thin Solid Films*, **1997**, 307**,** 221.
[11] NY Shishkin; IM Zharsky; VG Lugin. *Sens. Actuators*, **1998**, B 48, 403.
[12] NS Baik; G Sakai; N Miura. *Sens. Actuators*, **2000**, B 63, 74.
[13] F Gu; SF Wang; MK Lu. *J. Phys. Chem.*, **2004**, B 108, 8119.
[14] S Sindhu; MR Anantharaman; BU Thampi; KA Malini; P.Kurian. *Bull. Mater. Sci.*, **2002**, 25**,** 599.
[15] SG Pawar; SL Patil; AT Mane; BT Raut; V B Patil. *Arch. Appl. Sci. Res.*, **2009**, 1 (2), 109.
[16] MK Pal; B Singh; J Gautam. *Arch. Appl. Sci. Res*, **2009**, 1 (2), 313.
[17] SB Kondawar; SD Bompilwar; VS Khati; SR Thakre; VA Tabhane; DK Burghate. *Arch. Appl. Sci. Res*, **2010**, 2 (1), 247.
[18] CM Liu; XT Zu; WL Zhou. *J. Phys.: Condens. Matter*, **2006**, 18, 6001.

[19] A Punnoose; J Hays; A Thuber; MH Engelhard; RK Kukkadapu; C Wang; V Shutthanandan; S Thevuthasan. *Phys. Rev.*, **2005**, B 72, 54402.
[20] B Chen; J Sha; XS Ye; ZG Jiao; LD Zhang. *Science China*, **1999**, 42, 510.
[21] P Boguslawski; EL Briggs; Bernholc. *J. Phys. Rev. B*, **1995**, 51, 17255.
[22] P Perlin; T Suski; H Teisseyre. *Phys. Rev. Lett.*, **1995**, 75, 296.
[23] WY Wang; YP Xu; DF Zhang; XL Chen. *Mater. Res. Bull.*, **2001**, 36, 2155.
[24] YP Xu; WY Wang; DF Zhang; XL Chen. *J. Mater. Sci.*, **2001**, 36, 4401.
[25] H Frohlick, *Theory of Dielectrics*, Oxford University press, **1956**.
[26] M Ghosh; CNR Rao. *Chem. Phys. Lett.*, **2004**, 393, 493.
[27] AS Lanje; SJ Sharma; RB Pode. *Arch. Phy. Res.*, **2010**, 1(1), 49.